Journal of Computational Physics **170,** 550–561 (2001)
doi:10.1006/jcph.2001.6748, available online at http://www.idealibrary.com on IDEAL®

A New Unconditionally Stable Algorithm for Steady-State Fluid Simulation of High Density Plasma Discharge

Hee-Hwan Choe,* N. S. Yoon,† S. S. Kim,‡ and Duk-In Choi*

*Department of Physics, Korea Advanced Institute of Science and Technology, Taejon 305-701, Korea; †School of Electrical and Electronic Engineering, Chungbuk National University, Chungju Chungbuk 361-763, Korea; ‡Department of Fundamental Energy Science, Kyoto University, Uji, Kyoto 611-0011, Japan
E-mail: nsyoon@engine.chungbuk.ac.kr

Received October 23, 2000; revised January 27, 2001

A new unconditionally stable algorithm for steady-state fluid simulation of high density plasma discharge is suggested. The physical origin of restriction on simulation time step is discussed and a new method to overcome it is explained. To compare the new method with previous other methods, a one-dimensional fluid simulation of inductively coupled plasma discharge is performed.

Key Words: fluid; simulation; perturbation; numerical method.

1. INTRODUCTION

A lot of research on high density plasma discharges such as inductively coupled plasma (ICP), electron cyclotron resonance, and Helicon wave discharges is being conducted, because the progress in submicron electronic device fabrication demands a higher degree process optimization [1]. For transport modeling of high density plasma discharge, fluid simulation [2–4] has been extensively used to study discharge characteristics, because the global insight on the profiles of quantities such as densities, temperatures, fluxes, and potential can be obtained. But for a stable fluid simulation of high density plasma, there are severe restrictions on the time step (Δt) and the grid size (Δz), because the shielding time scale of an electric field perturbation is very short, and the sheath length is quite small.

For the grid size (Δz) limitation, there are several methods to manage the restriction (1) by modeling the sheath and plasma separately, and utilizing appropriate plasma-sheath boundary condition [4], (2) by utilizing upwind difference scheme, (3) by using exponential scheme [5], and so on. And for the time step (Δt) restriction, the maximum time step is concerned with various time scales: mean time of ionization and collision, particle and energy confinement time, Courant time step, inverse of plasma frequency (ω_p), and dielectric

0021-9991/01 $35.00

relaxation time (τ_d). The simulation time step using an explicit method cannot exceed the minimum value of those time scales. The most severe restriction is due to the ω_p^{-1} and τ_d [6]. As an example, for typical ICP discharge conditions, the minimum time step is the dielectric relaxation time $\sim 10^{-13}$ s, which is actually impractical. However, usually, the main purpose of fluid simulation of the high density plasma discharges is not in the description of a transient effect or wave excitations but in the achievement of steady-state values. In fluid simulation of steady state, it is desirable to take a time step close to Courant time step which is larger than ω_p^{-1} or τ_d.

Several methods to overcome the limitation on the simulation time step are suggested [2–4]. In [2, 3], they used time step larger than τ_d using a semiimplicit solution of Poisson's equation. However, as will be described in the next section, some more demands for improvement on the stability and the accuracy still remain.

Therefore, in this work, we suggest a new stable and accurate method by imitating a realistic, physical shielding process of electric field perturbation to overcome the dielectric limitation on time step. The new method is applied to a one-dimensional ICP discharge model, and the simulation results are compared with previous methods. Section 2 describes details of the new method, and Section 3 presents the simulation results using the present method compared with other methods.

2. DESCRIPTION OF THE NEW ALGORITHM

The usually adopted set of equations for fluid simulation of high density plasma discharges are the continuity, momentum, Poisson, and electron temperature equations.

$$\frac{\partial n_i}{\partial t} + \nabla \cdot \mathbf{\Gamma}_i = \nu_{\text{ion}} n_e, \tag{1}$$

$$\frac{\partial n_e}{\partial t} + \nabla \cdot \mathbf{\Gamma}_e = \nu_{\text{ion}} n_e, \tag{2}$$

$$\frac{\partial \mathbf{\Gamma}_i}{\partial t} = \frac{e n_i}{M}\mathbf{E} - \nu_i \mathbf{\Gamma}_i - \frac{1}{M}\nabla(n_i T_i), \tag{3}$$

$$\frac{\partial \mathbf{\Gamma}_e}{\partial t} = -\frac{e n_e}{m}\mathbf{E} - \nu_e \mathbf{\Gamma}_e - \frac{1}{m}\nabla(n_e T_e), \tag{4}$$

$$\nabla \cdot \mathbf{E} = 4\pi e\,(n_i - n_e)\,, \tag{5}$$

$$\frac{3}{2}\frac{\partial (n_e T_e)}{\partial t} = -\nabla \cdot \mathbf{Q} - e\mathbf{\Gamma}_e \cdot \mathbf{E} + P_{\text{ext}} - P_{\text{coll}}, \tag{6}$$

where $\mathbf{\Gamma}_i$ is ion flux, $\mathbf{\Gamma}_e$ is electron flux, n_i is ion density, n_e is electron density, ν_{ion} is the ionization collision frequency, M is ion mass, ν_i is ion neutral collision frequency, T_i is ion temperature, m is electron mass, ν_e is electron neutral collision frequency, T_e is electron temperature, P_{coll} is collisional power loss per volume, $\mathbf{Q}$ is electron energy flux, and P_{ext} is externally applied power per volume. Here the stress term in Eqs. (3) and (4) is neglected. For the electron momentum equation, we followed the procedure presented in [2, 3], and for the ion momentum equation, although we can include and calculate it directly, we exclude it for the sake of convenience in the development of the new method. When Eq. (5) is solved along with Eq. (2) in an explicit time integration scheme, the severe time step limitation occurs.

To overcome the limitation, we rearrange the given equations. Equations (1) and (2) give

$$\frac{\partial n}{\partial t} + \nabla \cdot \mathbf{\Gamma} = 0, \tag{7}$$

where $n = n_i - n_e$ and $\mathbf{\Gamma} = \mathbf{\Gamma}_i - \mathbf{\Gamma}_e$. Substitution of the time derivative of Poisson's equation to Eq. (7) gives

$$\nabla \cdot \left(\frac{\partial \mathbf{E}}{\partial t} + 4\pi e \mathbf{\Gamma} \right) = \nabla \cdot (4\pi \mathbf{J}_{\text{tot}}) = 0, \tag{8}$$

where $\mathbf{J}_{\text{tot}}$ is the total current density. Using the differential form of Faraday's law of electromagnetic induction, we can express the term in large parentheses as $\nabla \times (c\mathbf{B})$. In this work, we will develop a new method for overcoming the time step limitation for the case of the term in large parentheses, total current ($\mathbf{J}_{\text{tot}}$) being zero:

$$4\pi \mathbf{J}_{\text{tot}} = \nabla \times (c\mathbf{B}) = \frac{\partial \mathbf{E}}{\partial t} + 4\pi e \mathbf{\Gamma} = 0. \tag{9}$$

Since we are focusing on developing quantities which describe a plasma in steady state, we can assume that the time derivative of the electric field will be zero. And, by ambipolarity, the conduction current will also be zero: $\mathbf{\Gamma}_i = \mathbf{\Gamma}_e$ implies $\mathbf{\Gamma} = 0$. There, surely, exist cases where total current density is not zero. For instance, we can consider the case for the capacitive radio frequency discharge, where a net current across plasma exists. And when the direction of ion flux and that of the electron flux differ from each other, current generated by electrons and ions out of plasma, and flowing through the conducting chamber wall, exists, so $\mathbf{J}_{\text{tot}} \neq 0$. In this preliminary study, we only deal with the simple case, $\mathbf{J}_{\text{tot}} = 0$, and a method for managing $\mathbf{J}_{\text{tot}} \neq 0$ will be developed in future work.

In applying finite difference method (FDM) in time evolution, we have to integrate $\partial \mathbf{E}/\partial t + 4\pi e \mathbf{\Gamma} = 0$ during finite time step, Δt

$$\int_0^{\Delta t} \left[\frac{\partial \mathbf{E}}{\partial t} + 4\pi e \mathbf{\Gamma}(t) \right] = 0,$$

where $0 \leq t \leq \Delta t$. Then we have

$$\Delta \mathbf{E} = \mathbf{E}(\Delta t) - \mathbf{E}(0) = -4\pi e \int_0^{\Delta t} \mathbf{\Gamma}(t)\, dt, \tag{10}$$

$$\Delta \rho = \frac{1}{4\pi e} \nabla \cdot (\Delta \mathbf{E}), \tag{11}$$

where $\Delta \mathbf{E}$ and $\Delta \rho$ represent the time variation of electric field and charge density before and after simulation time step, respectively. The first idea of the present method is to replace the electron continuity equation with Eq. (11). First, we obtain the time variation of the electric field ($\Delta \mathbf{E}$) during a simulation time step. Second, we calculate the charge density variation ($\Delta \rho$) using Poisson's equation. And finally we get electron density change using $\Delta n_e = \Delta n_i - \Delta \rho$. The second idea lies in the method to obtain the FDM form of Eq. (10). In the explicit and implicit methods, $\mathbf{\Gamma}$ is assumed to be constant during the integration.

When the explicit method is used, by using $\mathbf{\Gamma}(t) = \Gamma(0)$, we have

$$\delta\mathbf{E}(t) = -4\pi e\mathbf{\Gamma}(0)t, \tag{12}$$

and for the implicit method, by applying $\mathbf{\Gamma}(t) = \mathbf{\Gamma}\Delta t)$, we get

$$\delta\mathbf{E}(t) = -4\pi e\mathbf{\Gamma}(\Delta t)t, \tag{13}$$

where $\delta\mathbf{E}(t)$ is the time variation of electric field during $0 \le t \le \Delta t$, and Δt is the simulation time step. Figure 1 shows $\delta\mathbf{E}(t)$ for three methods (explicit, implicit, and our method) with realistic physical damping of electric field perturbation whose relaxation time is τ. Basically, the explicit method uses the time derivative of the value at $t = 0$; if the derivative is large it would make a numerical problem. Thus this method is applicable when time step is much smaller τ: $\Delta t \ll \tau$. $\delta\mathbf{E}(t)$ in the explicit method is overestimated for time step larger than the relaxation time: $\Delta t > \tau$. The overestimation will change the sign of $\delta\mathbf{E}$ and cause numerical instability. On the other hand, since the implicit method uses time advancing $\mathbf{\Gamma}(\Delta t)$, it is numerically stable even if the simulation time step is larger than the relaxation time: $\Delta t > \tau$. But $\delta\mathbf{E}$ is underestimated; therefore the implicit method cannot assure the accuracy. Because the implicit method utilizes the time derivative of the value at $t = \Delta t$, for cases when the derivative is small, it will take a small value. To sum up, the explicit and implicit methods cannot achieve numerical stability or sufficient accuracy for large time step. We will develop a numerically stable and accurate method by imitating the physical shielding process of electric field perturbation.

We calculate the integral without the assumption that $\mathbf{\Gamma}$ is constant during integration. Let $\mathbf{\Gamma}_i(t) = \mathbf{\Gamma}_{i0} + \delta\mathbf{\Gamma}_i(t)$, $\mathbf{\Gamma}_e(t) = \mathbf{\Gamma}_{e0} + \delta\mathbf{\Gamma}_e(t)$, $\rho(t) = \rho_0 + \delta\rho(t)$, and let $\mathbf{E}(t) = \mathbf{E}_0 + \delta\mathbf{E}(t)$ during the simulation time step, $0 \le t \le \Delta t$. Here subscript "0" indicates values before time evolution of quantities, and "δ" represents the time variation of quantities

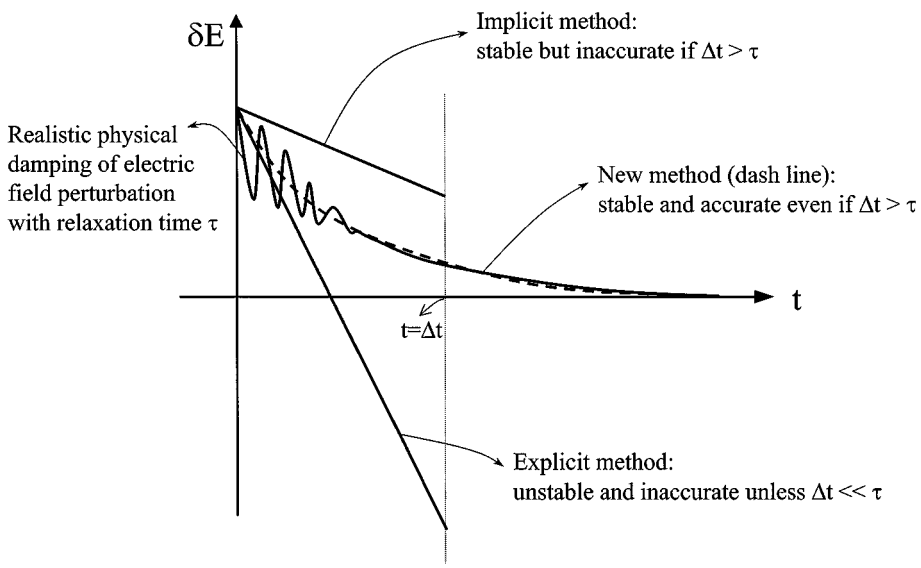

FIG. 1. Illustration showing physical change of electric perturbation and numerically calculated values for various methods.

during simulation time step. If the electric field is dealt with implicitly, and densities and temperatures are treated explicitly, then momentum equations become

$$\frac{\partial(\delta\mathbf{\Gamma}_i)}{\partial t} = \frac{\omega_i^2}{4\pi e}\delta\mathbf{E} - \nu_i\delta\mathbf{\Gamma}_i, \tag{14}$$

$$\frac{\partial(\delta\mathbf{\Gamma}_e)}{\partial t} = -\frac{\omega_e^2}{4\pi e}\delta\mathbf{E} - \nu_e\delta\mathbf{\Gamma}_e (0 \le t \le \Delta t), \tag{15}$$

where ω_i and ω_e are ion and electron plasma frequencies respectively. And $\partial\mathbf{E}/\partial t + 4\pi e\mathbf{\Gamma} = 0$ becomes

$$\frac{\partial\delta\mathbf{E}(t)}{\partial t} = -4\pi e\,[\mathbf{\Gamma}_0 + \delta\mathbf{\Gamma}(t)] \quad (0 \le t \le \Delta t), \tag{16}$$

where $\mathbf{\Gamma}_0 = \mathbf{\Gamma}_{i0} - \mathbf{\Gamma}_{e0}$ and $\delta\mathbf{\Gamma}(t) = \delta\mathbf{\Gamma}_i(t) - \delta\mathbf{\Gamma}_e(t)$. The time variation of charge density is

$$\delta\rho(t) = \frac{1}{4\pi e}\nabla\cdot(\delta\mathbf{E}(t)). \tag{17}$$

Solving Eqs. (14) and (15), we have

$$\delta\mathbf{\Gamma}_i = \frac{\omega_i^2}{4\pi e}\exp(-\nu_i t)\int_0^t \exp(\nu_i\xi)\delta\mathbf{E}(\xi)d\xi, \tag{18}$$

$$\delta\mathbf{\Gamma}_e = -\frac{\omega_e^2}{4\pi e}\exp(-\nu_e t)\int_0^t \exp(\nu_e\xi)\delta\mathbf{E}(\xi)d\xi \quad (0 \le t \le \Delta t). \tag{19}$$

Equations (16), (18), and (19) yield

$$\frac{\partial\delta\mathbf{E}}{\partial t} = -4\pi e\mathbf{\Gamma}_0 + \int_0^t \left[\frac{e^{-\nu_e(t-\xi)}}{\tau_e} + \frac{e^{-\nu_i(t-\xi)}}{\tau_i} - \frac{1}{\tau_d}\right]\frac{\partial\delta\mathbf{E}}{\partial\xi}d\xi, \tag{20}$$

where $\tau_e = \nu_e/\omega_e^2$, $\tau_i = \nu_i/\omega_i^2$, and $1/\tau_d = 1/\tau_e + 1/\tau_i$. It is noticeable that the process of reaching Eq. (20) is similar to that of obtaining the exponential scheme [5] which is used for removing grid size restriction. Equation (20) is the Volterra equation of special type because the kernel in the equation depends only on the difference of the two arguments, $t - \xi$.

Two initial conditions for $\delta\mathbf{E}$ are required to solve Eq. (20), and it is given by

$$[\delta\mathbf{E}]_{t=0} = 0\,, \quad \left[\frac{\partial\delta\mathbf{E}}{\partial t}\right]_{t=0} = -4\pi e\mathbf{\Gamma}_0. \tag{21}$$

Afte r some algebra, the solution of Eq. (20) becomes

$$\delta\mathbf{E}(t) = -4\pi e\mathbf{\Gamma}_0\left[\tau_d + \sum_{k=1}^{3}\frac{R_k}{s_k^2}\exp(s_k t)\right], \tag{22}$$

where

$$R_{1,2,3} = \frac{[(\tau_e\nu_i + \tau_i\nu_e)s_{1,2,3} + (\tau_e + \tau_i)\nu_e\nu_i][s_{2,3,1} - s_{3,1,2}]}{\tau_i\tau_e(s_1 - s_2)(s_2 - s_3)(s_3 - s_1)},$$

and $s_{1,2,3}$ are the zeros of

$$s^3 + (\nu_e + \nu_i)s^2 + \left(\nu_e\nu_i + \frac{\nu_e}{\tau_i} + \frac{\nu_i}{\tau_e}\right)s + \left(\frac{1}{\tau_e} + \frac{1}{\tau_i}\right)\nu_e\nu_i = 0.$$

This equation predicts electric field of future time. We can simplify Eq. (22) for two cases.

First, if collision frequencies ν_e and ν_i are sufficiently large that the two exponential terms in Eq. (20) can be neglected, then Eq. (22) becomes

$$\delta\mathbf{E}(t) = -4\pi e\mathbf{\Gamma}_0\tau_d\left[1 - \exp\left(-\frac{t}{\tau_d}\right)\right]. \tag{23}$$

Second, utilizing the fact that $\omega_i \ll \omega_e$ implies $\tau_e \ll \tau_i$, we can neglect the second term in the integrand in Eq. (20). In this case, we have

$$\delta\mathbf{E}(t) = -4\pi e\mathbf{\Gamma}_0\left[\tau_d + \frac{R_1}{s_1^2}\exp(s_1 t) + \frac{R_2}{s_2^2}\exp(s_2 t)\right], \tag{24}$$

where

$$1/\tau_c = \nu_e + 1/\tau_i,$$

$$R_{1,2} = \pm\frac{(\tau_d - \tau_e)s_{1,2} - \tau_e\nu_e}{\tau_d\tau_e(s_1 - s_2)},$$

and

$$s_{1,2} = \frac{-1/\tau_c \pm \sqrt{1/\tau_c^2 - 4\nu_e/\tau_d}}{2}.$$

The $\delta\mathbf{E}$ in Eq. (24) can be classified by collision dominance.

(1) If $\nu_e \geq 2\omega_e + 1/\tau_i$, when the collision is dominant, $s_{1,2}$ is real and negative. Since the collision frequency is large in this case, $\delta\mathbf{E}$ eventually comes to that in Eq. (23). This case of high collision frequency can be found in plasmas display panels: $T_e \sim 4\,\text{eV}$, $n_e \sim 10^{11}\text{cm}^{-3}$, and gas pressure is hundreds of Torr, which imply $2\omega_e \leq \nu_e - 1/\tau_i$.

(2) If $\nu_e < 2\omega_e + 1/\tau_i$, when collision is not dominant, $\delta\mathbf{E}$ is expressed as

$$\delta\mathbf{E}(t) = -4\pi e\mathbf{\Gamma}_0\left[\tau_d + 2\left|\frac{R_1}{s_1^2}\right|\cos(\xi t + \theta)\exp\left(-\frac{t}{\tau_c}\right)\right], \tag{25}$$

where $\xi = 2\omega_e\sqrt{1 - ([\nu_e + 1/\tau_e - 1/\tau_d]/2\omega_e)^2}$, $\theta = \arg(R_1/s_1^2)$. This is the case when the collision is not dominant. This is applicable for typical ICP discharge conditions. The oscillation term in Eq. (25) appears to be due to the imaginary part of $s_{1,2}$, and its oscillation frequency ξ depends on plasma frequency, electron neutral collision frequency, and dielectric relaxation time which characterize the relaxation time scale of electric field. That is, ξ reflects the transient effects. Since we give our attention not to the transient effect but to steady state, we trace the oscillation center. This can be achieved by setting $\cos(\xi\Delta t + \theta)$ to $\cos(\theta)$. Actually, it does not matter in simulation if we adopt $\Delta t \gg \tau_c$, which implies the second term in the parentheses goes to zero. Summarizing, we have solved Eq. (16); if the collision is dominant, the solution is given in Eq. (23). In this case the relaxation time scale of the electric field is the dielectric relaxation time. If the collision is not dominant, the solution is given by Eq. (25), and in this case the relaxation time scale of electric field is ν_e^{-1} and τ_i.

Finally, since $\delta\mathbf{E}(t)$ is calculated, $\Delta\mathbf{E}$, $\Delta\rho$, and Δn_e are given by

$$\Delta\mathbf{E} = \delta\mathbf{E}(\Delta t), \tag{26}$$

$$\Delta\rho = \frac{1}{4\pi e}\nabla\cdot(\Delta\mathbf{E}), \tag{27}$$

$$\Delta n_e = \Delta n_i - \Delta\rho, \tag{28}$$

where Δ is the difference of values before and after simulation time step. The flow chart of the new method is given in Fig. 2. The main algorithm is the substitution of the electron continuity equation as follows: We calculate successively (1) the time variation of electric field ($\Delta\mathbf{E}$) using Eq. (22), (2) the time variation of charge density using $\Delta\rho = \nabla\cdot(\Delta\mathbf{E})/(4\pi e)$, and (3) the time variation of electron density using $\Delta n_e = \Delta n_i - \Delta\rho$.

Therefore the new method overcoming the time step limitation is developed and is unconditionally stable. It is noticeable that the procedure for making a finite difference form in the new method resembles that in exponential scheme [5].

3. ONE-DIMENSIONAL FLUID SIMULATION RESULTS AND DISCUSSIONS

As an example application of the present method, a one-dimensional fluid simulation of Ar plasma discharge is performed. The fluid equations for describing this case are

$$\frac{\partial n_i}{\partial t} = -\frac{\partial \Gamma_i}{\partial z} + R_{\mathrm{iz}}, \tag{29}$$

$$\frac{\partial E}{\partial z} + 4\pi e\Gamma = 0 \tag{30}$$

$$\frac{\partial \Gamma_i}{\partial t} = \frac{en_i}{M}E - \nu_i\Gamma_i - \frac{1}{M}\frac{\partial(n_i T_i)}{\partial z}, \tag{31}$$

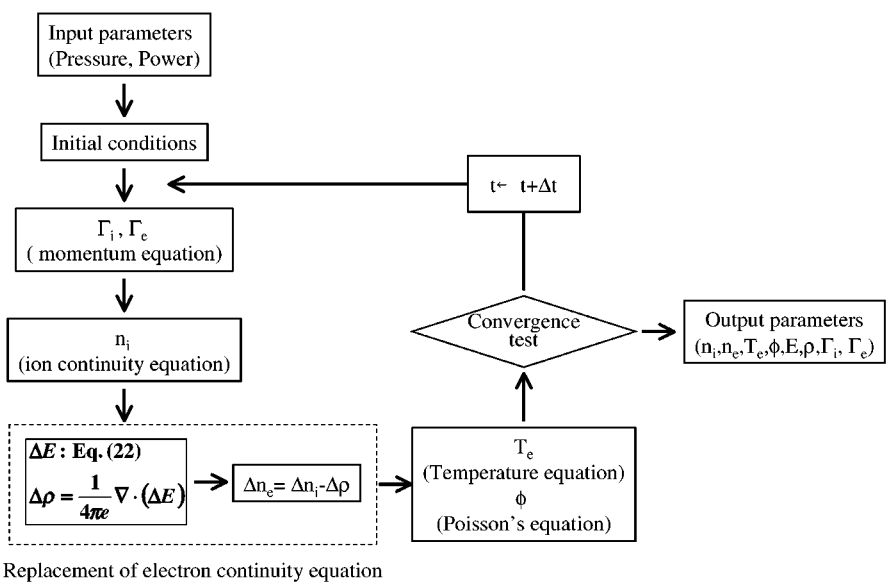

FIG. 2. Schematic diagram (flow chart) of algorithm.

$$\frac{\partial \Gamma_e}{\partial t} = -\frac{en_e}{m}E - \nu_e \Gamma_e - \frac{1}{m}\frac{\partial (n_e T_e)}{\partial z}, \tag{32}$$

$$\frac{\partial E}{\partial z} = 4\pi e\,(n_i - n_e)\,, \tag{33}$$

$$\frac{3}{2}\frac{\partial (n_e T_e)}{\partial t} = -\frac{\partial Q}{\partial z} - e\Gamma_e E + P_{\text{ext}} - P_{\text{coll}}, \tag{34}$$

where R_{iz} is the ionization rate per volume and other variables are mentioned in previous section. We can see that electron continuity equation is replaced with $J_{\text{tot}} = 0$. Since our method is not sensitive to boundary conditions, we take simple boundary conditions: $\phi = 0$, $n_e = 0$, $n_i = 0$, $\partial T_e/\partial z = 0$, and $\partial \Gamma_{i,e}/\partial z = 0$.

In the finite difference expression of fluxes, we applied an exponential scheme [7] because it provides numerically stable estimates of the particle flux. Finite difference forms become

$$\frac{n_{i,k}^{n+1} - n_{i,k}^{n}}{\Delta t} = -\frac{\Gamma_{i,k+1/2}^{n} - \Gamma_{i,k-1/2}^{n}}{\Delta z} + R_k, \tag{35}$$

$$\begin{aligned}\Delta E_{k+1/2}^{n+1} = {} & -4\pi e\left(\Gamma_{i,k+1/2}^{n} - \Gamma_{e,k+1/2}^{n}\right) \\ & \times \left[\tau_{d,k+1/2} + 2\left|\frac{R_{1,k+1/2}}{s_{1,k+1/2}^{2}}\right|\cos(\theta_{k+1/2})\exp\left(-\frac{\Delta t}{\tau_{c,k+1/2}}\right)\right],\end{aligned} \tag{36}$$

$$\Delta \rho_k^{n+1} = \frac{1}{4\pi e}\frac{\Delta E_{k+1/2}^{n+1} - \Delta E_{k-1/2}^{n+1}}{\Delta z} \tag{37}$$

$$n_{e,k}^{n+1} = n_{e,k}^{n} + n_{i,k}^{n+1} - n_{i,k}^{n} - \Delta \rho_k^{n+1}, \tag{38}$$

$$\begin{aligned}&\Gamma_{i,k+1/2}^{n+1} + \frac{1}{\nu_{i,k+1/2}}\frac{\Gamma_{i,k+1/2}^{n+1} - \Gamma_{i,k+1/2}^{n}}{\Delta t} \\ &\quad = A_{i,k+1/2}\left[\frac{p_{i,k+1/2}}{1 - \exp(p_{i,k+1/2})}n_{i,k+1}^{n} - \frac{p_{i,k+1/2}\exp(p_{i,k+1/2})}{1 - \exp(p_{i,k+1/2})}n_{i,k}^{n}\right],\end{aligned} \tag{39}$$

$$\begin{aligned}&\Gamma_{e,k+1/2}^{n+1} + \frac{1}{\nu_{e,k+1/2}}\frac{\Gamma_{e,k+1/2}^{n+1} - \Gamma_{e,k+1/2}^{n}}{\Delta t} \\ &\quad = A_{e,k+1/2}\left[\frac{p_{e,k+1/2}}{1 - \exp(p_{e,k+1/2})}n_{e,k+1}^{n} - \frac{p_{e,k+1/2}\exp(p_{e,k+1/2})}{1 - \exp(p_{e,k+1/2})}n_{e,k}^{n}\right],\end{aligned} \tag{40}$$

$$\frac{\phi_{k+1}^{n+1} - 2\phi_k^{n+1} + \phi_{k-1}^{n+1}}{(\Delta z)^2} = -4\pi e\left(n_{i,k}^{n+1} - n_{e,k}^{n+1}\right) \tag{41}$$

$$\begin{aligned}\frac{T_{e,k}^{n+1} - T_{e,k}^{n}}{\Delta t} = {} & \frac{T_{e,k}^{n+1}}{3}\frac{u_{k+1/1} - u_{k-1/2}}{\Delta z} - \frac{u_{k+1/2}T_{e,k+1/2}^{n+1} - u_{k-1/2}T_{e,k-1/2}^{n+1}}{\Delta z} \\ & - \frac{2}{3n_{e,k}^{n}}\left(\frac{\partial q}{\partial z}\right)_k + \frac{2}{3}\frac{P_{\text{ext},k} - P_{\text{coll},k}}{n_{e,k}^{n}} - \frac{R_k}{n_{e,k}^{n}}T_{e,k}^{n+1},\end{aligned} \tag{42}$$

where subscript k or $k + 1/2$ indicate space grid location, superscript n implies current time

level variables, $n+1$ stands for the future time level variables to be solved for, and Δ in E or ρ means difference of values between time steps $n+1$ and n.

And

$$
\begin{aligned}
(\partial q/\partial z)_k &= -5\{n^n_{e,k+1/2}T^n_{e,k+1/2}\big(T^{n+1}_{e,k+1}-T^{n+1}_{e,k}\big)/\Delta z - n^n_{e,k-1/2}T^n_{e,k-1/2}\\
&\quad\times\big(T^{n+1}_{e,k}-T^{n+1}_{e,k-1}\big)/\Delta z\}/(2m\nu_k\Delta z),\\
A_{i,k+1/2} &= T_i/M\nu_{i,k+1/2}\Delta z,\\
p_{i,k+1/2} &= eE_{k+1/2}\Delta z/T_i,\\
A_{e,k+1/2} &= T_{e,k+1/2}/m\nu_{e,k+1/2}\Delta z,\\
p_{e,k+1/2} &= -eE_{k+1/2}\Delta z/T_{e,k+1/2},
\end{aligned}
$$

and

$$u_{k+1/2} = \Gamma_{e,k+1/2}/n_{e,k+1/2}.$$

We assume that, as is usual for the ICP discharge, the local power deposition profile is $P_{\text{ext}} = P_0\exp(-2z/\delta)$, where δ is a skin depth; the ionization rate is $R_{\text{iz}} = \nu_{\text{iz}}n_e$, where $\nu_{\text{iz}} = n_N\sigma_{\text{iz}}v_e(T_e)\exp(-\epsilon_{\text{iz}}/T_e)$. Here n_N is neutral gas density, σ_{iz} is constant, v_e is electron mean thermal speed, and ϵ_{iz} is the ionization energy.

For comparison with other method, we considered a semiimplicit method [2] as follows. Poisson's equation at the future time level is

$$\left(\frac{\partial^2\phi^{n+1}}{\partial z^2}\right)_k = -4\pi e\left(n_i^{n+1}-n_e^{n+1}\right)_k. \tag{43}$$

The finite difference form of electron density equation can be written as

$$n^{n+1}_{e,k} = n^n_{e,k} + \Delta t\left(\frac{\partial n_{e,k}}{\partial t}\right),$$

and $(\partial n_{e,k}/\partial t)$ is obtained from time advanced potential:

$$\left(\frac{\partial n_{e,k}}{\partial t}\right) = -\frac{e}{m\nu_e}\frac{\partial}{\partial z}\left[n_e^n\frac{\partial\phi^{n+1}}{\partial z}\right]_k + \left[\frac{1}{m\nu_e}\frac{\partial^2\big(n_e^nT_e^n\big)}{\partial z^2}\right]_k + R_{\text{iz},k}.$$

When obtaining n_i^{n+1}, we did not use time advanced potential. The substitution of n_i^{n+1}, n_e^{n+1} into Eq. (43) gives

$$\big(1+4\pi e\Delta t\mu_e n_e^n\big)_k\left[\frac{\partial^2\phi^{n+1}}{\partial z^2}\right]_k + 4\pi e\Delta t\left[\mu_e\left(\frac{\partial n_e^n}{\partial z}\right)\left(\frac{\partial\phi^{n+1}}{\partial z}\right)\right]_k \tag{44}$$

$$= -4\pi e\left(n_i^{n+1}-n_e^n\right)_k + 4\pi e\Delta t\left[\frac{1}{m\nu_e}\frac{\partial^2\big(n_e^nT_e^n\big)}{\partial z^2} + R_{iz}\right]_k, \tag{45}$$

where $\mu_e = e/m\nu_e$. Solving this equation we could obtain ϕ_k^{n+1}. In the semiimplicit method, the time derivative of electron flux is neglected.

Figure 3 shows profiles of electron density, potential, and temperature under 10 mTorr, 500 W. 500 mesh is used in Fig. 3. The maximum allowed time step for stable solution is 10^{-11} for the semiimplicit method and 5×10^{-10} s for the new method. The simulation

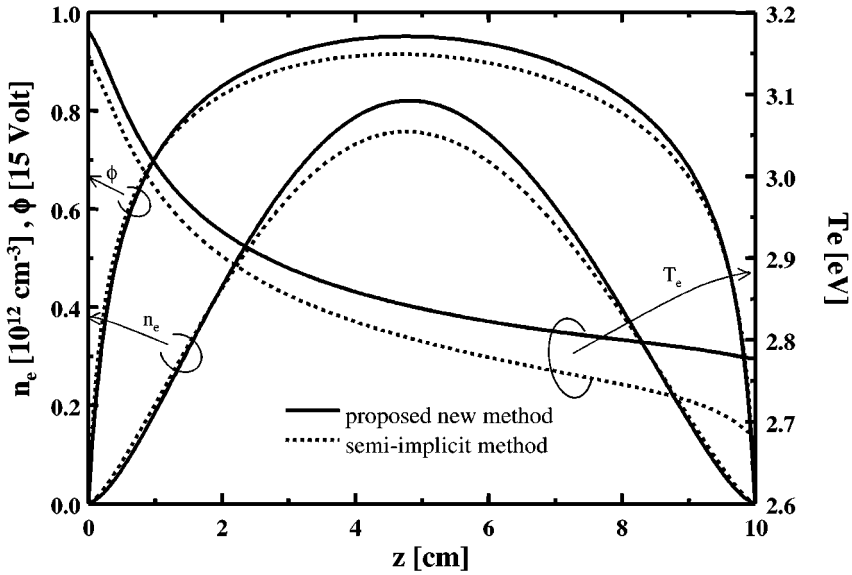

FIG. 3. Electron density (n_e), potential (ϕ), and electron temperature (T_e) profiles for a pressure of 10 *m*Torr and 500 W Ar plasma: Solid line for proposed method and dashed line for semiimplicit method.

time step depends on the number of mesh points used. For example, when 30 mesh points are used, Δt for the semiimplicit method is 10^{-9} s and for the new method is 10^{-8} s. This dependence of time step on mesh points is due to Courant time step. For simulation conditions, if $v \sim 10^7$ cm/s and $\Delta z \sim 10/N$ cm, where N is the number of mesh points, then the Courant time step is about 10^{-8} s for 30 mesh points and 10^{-9} s for 500 mesh points. Comparison between two methods yields good agreement in profile even though maximum time step for stable solution in the new method is about 10 times larger than that in the semiimplicit method.

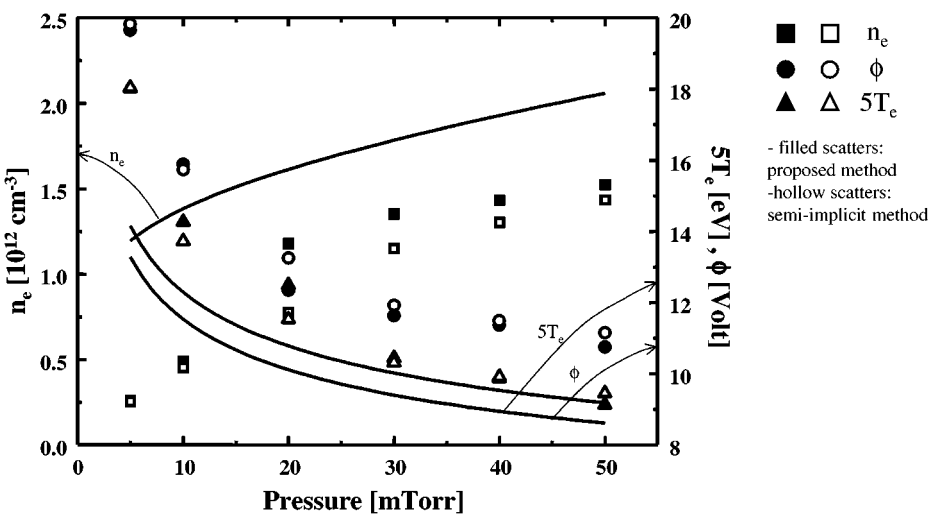

FIG. 4. Electron density (n_e, square), potential (ϕ, circle), and electron temperature (T_e, triangle) vs pressure for 500 W: Solid line for global modeling, filled scatters for proposed method, and hollow scatters for semiimplicit method.

Figure 4 shows electron density and temperature, and potential for various pressures and 500 W power. The real line is obtained from a global model [8] and the scatter data from fluid simulations: filled scatters correspond to the proposed method, and hollow scatters correspond to the semiimplicit method. All three parameters for pressures are in good agreement among the three methods. The simulation time step for the new method is larger than that for the semiimplicit method by several orders of magnitude. In spite of larger time step, the two methods show almost the same results. Global modeling results in the same qualitative trends as the other two methods with some differences in quantities.

4. CONCLUSIONS

We developed a new method to overcome the dielectric relaxation time restriction in steady-state fluid simulation of high density plasma discharges when the local ambipolarity is satisfied. The new method is successfully developed based on (1) replacement of electron continuity equation with differential form of Faraday's law of induction for cases when $\mathbf{J}_{\text{tot}} = 0$ and (2) imitating the physical shielding process of electric perturbation. It was discussed that the present method is unconditionally stable and more accurate than any implicit method.

The exponential method [7] gives numerically stable estimates of particle flux even though the voltage between mesh points is compatible or larger than the characteristic energy D/μ (D is the diffusion coefficient and μ is the mobility), and thus it enables us to use the large mesh size. However, there still remains the restriction on the time step in the application of the exponential scheme alone. The new method provides stable values of electron density although the simulation time step is larger than the dielectric relaxation time step; Δt is restricted only by Courant time step in the new method. Application of the new method to the fluid simulation without the exponential method needs the fine mesh size, and this allows the small simulation time step because the fine mesh size makes Courant time step small. By using both the exponential method for the large mesh size and the new method for the large time step, we could save much computation time, because the larger mesh size gives the larger Courant time step, which permits the larger simulation time step. And the results using the new method with the exponential method are in good agreement with those using semiimplicit method. Although the method in this paper is developed only for cases when the local ambipolarity is satisfied ($\mathbf{J}_{\text{tot}} = 0$) and applicable for such cases, the simplified model provides fundamental ideas to manage the time step restriction by replacing the electron continuity equation. For more general application, the development of methods for cases when the total current density exists will be done in future work.

ACKNOWLEDGMENTS

This work was supported by the Ministry of Science and Technology (MOST) and the Ministry of Commerce, Industry, and Energy (MOCIE) under the SYSTEM IC 2010 project contract.

REFERENCES

1. M. A. Lieberman and R. A. Gottscho, Design of high-density plasma sources for material processing, in *Physics of Thin Films*, edited by M. H. Francombe and J. L. Vossen, (Academic Press, New York, 1994), Vol. 18.

2. R. A. Stewart, P. Vitello, and D. B. Graves, *J. Vac. Sci. Technol. B* **12(1)**, 478 (1994).
3. P. L. G. Ventzek, R. J. Hoekstra, and M. J. Kushner, *J. Vac. Sci. Technol. B* **12**(1), 461 (1994).
4. N. S. Yoon, Nak-Heon Choi, Hyoung-Bin Park, and Duk-In Choi, *IEEE Trans. Plasma Sci.* **23**(4), 461 (1995).
5. S. V. Patankar, *Numerical Heat Transfer and Fluid Flow* (McGraw-Hill, New York, 1980).
6. M. S. Barnes, T. J. Colter, and M. E. Elta, *J. Appl. Phys.* **61**(1), 81 (1987).
7. J.-P. Boeuf, *Phys. Rev. A* **36**(6), 2782 (1987).
8. N. S. Yoon, S. S. Kim, C. S. Chang, and Duk-In Choi, *J. Korean Phys. Soc*. **28**(2), 172 (1996).